Excitation energies from time-dependent density-functional theory beyond the adiabatic approximation

C. A. Ullrich[a)]
Department of Physics, University of Missouri-Rolla, Rolla, Missouri 65409

Kieron Burke
Department of Chemistry and Chemical Biology, Rutgers University, Piscataway, New Jersey 08854

(Received 8 March 2004; accepted 8 April 2004)

Time-dependent density-functional theory in the adiabatic approximation has been very successful for calculating excitation energies in molecular systems. This paper studies nonadiabatic effects for excitation energies, using the current–density functional of Vignale and Kohn [Phys. Rev. Lett. **77**, 2037 (1996)]. We derive a general analytic expression for nonadiabatic corrections to excitation energies of finite systems and calculate singlet $s\rightarrow s$ and $s\rightarrow p$ excitations of closed-shell atoms. The approach works well for $s\rightarrow s$ excitations, giving a small improvement over the adiabatic local-density approximation, but tends to overcorrect $s\rightarrow p$ excitations. We find that the observed problems with the nonadiabatic correction have two main sources: (1) the currents associated with the $s\rightarrow p$ excitations are highly nonuniform and, in particular, change direction between atomic shells, (2) the so-called exchange-correlation kernels of the homogeneous electron gas, f_{xc}^{L} and f_{xc}^{T}, are incompletely known, in particular in the high-density atomic core regions. © *2004 American Institute of Physics.* [DOI: 10.1063/1.1756865]

I. INTRODUCTION

Time-dependent density-functional theory (TDDFT)[1,2] has become a popular tool for calculating excitation energies[3–5] of complex molecular systems,[6] including systems of biochemical interest[7,8] (see also Ref. 9 for an overview of recent applications). Almost all present applications of TDDFT employ the adiabatic approximation for time-dependent exchange-correlation (xc) effects: in constructing the xc potential at time t, all functional dependence of the time-dependent density prior to t is ignored. In the linear-response regime, this implies frequency-independent and real xc kernels. The simplest of these is the adiabatic local-density approximation (ALDA).[10]

There have been several attempts to construct a TDDFT approach beyond the ALDA. Gross and Kohn suggested using the frequency-dependent xc kernel of the uniform electron gas,[11] but this was was shown to violate the harmonic potential theorem.[12] Vignale and Kohn (VK)[13] showed that a nonadiabatic local approximation requires the time-dependent current as the basic variable, rather than the density. This formalism was later cast in a physically more transparent form by Vignale, Ullrich, and Conti (VUC),[14] using the language of hydrodynamics: nonadiabatic xc effects manifest themselves as viscoelastic stresses in the electron liquid. A detailed account of the VK/VUC functionals is available in Ref. 15.

The first application of the VUC formalism was to calculate linewidths of intersubband plasmons in semiconductor quantum wells.[16,17] These intersubband plasmons are collective electronic excitations with frequencies in the far-infrared. In the absence of disorder and phonon scattering, ALDA would give infinitely sharp plasmon lines, ignoring damping due to electronic many-body effects. This effect is included in the VUC formalism, with good quantitative agreement with experimental linewidth data.[17] We also mention an application of the VUC formalism for Hooke's atom with a time-periodic force constant.[18]

Van Faassen *et al.* recently used the VUC formalism to calculate static axial polarizabilities in molecular chains,[19,20] which are greatly overestimated within the ALDA. For many systems, a significant improvement over ALDA was achieved, in excellent agreement with *ab initio* quantum chemical methods. On the other hand, no improvement was obtained for hydrogen chains with alternating bond lengths, which can be viewed as a model for conjugated polymers.

The VUC formalism is thus showing considerable promise for modeling nonadiabatic effects in applications of TDDFT, but there are still many open questions: For what systems can nonadiabatic effects be expected to be important, and when is the VUC formalism applicable and successful? What are the reasons for failures of the VUC formalism, and what are the possible remedies?

The purpose of the present paper is twofold. We derive a simplified procedure for calculating excitation energies from current–TDDFT within the VUC approximation. This is an extension of the so-called small-matrix approximation (SMA).[5] The resulting analytic expression yields an intuitive interpretation of nonadiabatic effects in terms of energy dissipation in the viscous electron liquid.

We then test our formalism and calculate singlet $s\rightarrow s$ and $s\rightarrow p$ excitation energies in closed-shell atoms and ions. Formally, VUC is justified for systems with slowly varying densities and currents such as quantum wells and long mo-

a)Electronic mail: ullrichc@umr.edu

lecular chains, where it gives sensible results. However, to test its usefulness for molecular calculations, one needs to apply and analyze the VUC approximation in situations with rapidly varying ground-state densities and current responses, such as in atomic systems. We find that VUC breaks down for certain atomic $s\rightarrow p$ excitations, and our SMA analytic expression allows us to perform a detailed diagnosis of the problems.

We note that the SMA as well as its simplified version, the so-called single-pole approximation,[4] are justified for excitations involving states that are energetically well separated from the rest of the spectrum.[5] This is the case for low-lying atomic states, but is often not true in larger systems or in the presence of near-degeneracies.[21] In practice, full TDDFT calculations of excitation energies beyond the SMA[3] are feasible even for large molecules.

This paper is organized as follows: Section II contains an overview of linear current–density response theory, and a derivation of an analytic expression for nonadiabatic corrections to ALDA excitation energies. Numerical results, together with an analysis of the performance of the VUC functional, are presented in Sec. III. We give our conclusions in Sec. IV. We use Hartree atomic units ($e=m=\hbar=1$) unless indicated otherwise.

II. FORMALISM

A. Linear current–density response within and beyond the adiabatic approximation

We consider systems that are everywhere nonmagnetic, such as closed-shell atoms or molecules, and we consider only singlet excitations. The spin degree of freedom is therefore ignored. In TDDFT, the linear current–density response $\mathbf{j}(\mathbf{r},\omega)$ to an external, frequency-dependent vector potential $\mathbf{a}^{\mathrm{ext}}(\mathbf{r},\omega)$ is given by

$$j_\mu(\mathbf{r},\omega)=\sum_\nu \int d^3r'\,\chi_{\mu\nu}(\mathbf{r},\mathbf{r}',\omega)[a_\nu^{\mathrm{ext}}(\mathbf{r}',\omega)+a_\nu^{\mathrm{H}}(\mathbf{r}',\omega)+a_\nu^{\mathrm{xc}}(\mathbf{r}',\omega)], \tag{1}$$

where μ and ν denote Cartesian coordinates. Equation (1) features the noninteracting (Kohn–Sham) current–current response tensor $\chi_{\mu\nu}$, defined as

$$\chi_{\mu\nu}(\mathbf{r},\mathbf{r}',\omega)=n_0(\mathbf{r})\,\delta(\mathbf{r}-\mathbf{r}')\,\delta_{\mu\nu}+R_{\mu\nu}(\mathbf{r},\mathbf{r}',\omega). \tag{2}$$

n_0 is the ground-state density, and the paramagnetic part of the response tensor is

$$R_{\mu\nu}(\mathbf{r},\mathbf{r}',\omega)=\frac{1}{2}\sum_{j,k}^{\infty}\frac{f_k-f_j}{\varepsilon_k-\varepsilon_j+\omega+i\eta}\times[\psi_k^*(\mathbf{r})\nabla_\mu\psi_j(\mathbf{r})-\psi_j(\mathbf{r})\nabla_\mu\psi_k^*(\mathbf{r})]\times[\psi_j^*(\mathbf{r}')\nabla'_\nu\psi_k(\mathbf{r}')-\psi_k(\mathbf{r}')\nabla'_\nu\psi_j^*(\mathbf{r}')]. \tag{3}$$

The noninteracting density–density response function

$$\chi(\mathbf{r},\mathbf{r}',\omega)=2\sum_{j,k}^{\infty}(f_k-f_j)\frac{\psi_k^*(\mathbf{r})\psi_j(\mathbf{r})\psi_k(\mathbf{r}')\psi_j^*(\mathbf{r}')}{\varepsilon_k-\varepsilon_j+\omega+i\eta} \tag{4}$$

is related to $\chi_{\mu\nu}$ as follows:

$$\chi(\mathbf{r},\mathbf{r}',\omega)=\frac{1}{\omega^2}\sum_{\mu\nu}\nabla_\mu\nabla'_\nu\chi_{\mu\nu}(\mathbf{r},\mathbf{r}',\omega). \tag{5}$$

j_μ is calculated in Eq. (1) as the current–density response of a noninteracting system to an effective vector potential. The many-body effects enter through the linearized Hartree vector potential

$$a_\nu^{\mathrm{H}}(\mathbf{r},\omega)=\frac{\nabla_\nu}{(i\omega)^2}\int d^3r'\frac{\nabla'\cdot\mathbf{j}(\mathbf{r}',\omega)}{|\mathbf{r}-\mathbf{r}'|}, \tag{6}$$

and through the xc vector potential $a_\nu^{\mathrm{xc}}(\mathbf{r},\omega)$. The simplest approximation for a_ν^{xc} is the ALDA, which is defined as

$$a_\nu^{\mathrm{xc,ALDA}}(\mathbf{r},\omega)=\frac{\nabla_\nu}{(i\omega)^2}\int d^3r'\nabla'\cdot\mathbf{j}(\mathbf{r}',\omega)f_{\mathrm{xc}}^{\mathrm{ALDA}}(\mathbf{r},\mathbf{r}'), \tag{7}$$

where

$$f_{\mathrm{xc}}^{\mathrm{ALDA}}(\mathbf{r},\mathbf{r}')=\left.\frac{d^2e_{\mathrm{xc}}}{dn^2}\right|_{n=n_0(\mathbf{r})}\delta(\mathbf{r}-\mathbf{r}') \tag{8}$$

is the frequency-independent ALDA xc kernel (e_{xc} is the xc energy density of a homogeneous electron gas). Combining this with the integral kernel of the Hartree term (6), we define

$$f_{\mathrm{Hxc}}^{\mathrm{ALDA}}(\mathbf{r},\mathbf{r}')=\frac{1}{|\mathbf{r}-\mathbf{r}'|}+f_{\mathrm{xc}}^{\mathrm{ALDA}}(\mathbf{r},\mathbf{r}'). \tag{9}$$

In contrast with the xc scalar potential, the xc vector potential admits a frequency-dependent local approximation.[13–15] The resulting expression can be written as follows:

$$a_\nu^{\mathrm{xc}}(\mathbf{r},\omega)=a_\nu^{\mathrm{xc,ALDA}}(\mathbf{r},\omega)-\frac{1}{i\omega n_0(\mathbf{r})}\sum_\kappa\nabla_\kappa\sigma_{\nu\kappa}^{\mathrm{xc}}(\mathbf{r},\omega). \tag{10}$$

Here, $\sigma_{\nu\kappa}^{\mathrm{xc}}$ is the xc viscoelastic stress tensor:

$$\sigma_{\nu\kappa}^{\mathrm{xc}}=\eta_{\mathrm{xc}}(\nabla_\nu u_\kappa+\nabla_\kappa u_\nu-\tfrac{2}{3}\nabla\cdot\mathbf{u}\delta_{\nu\kappa})+\zeta_{\mathrm{xc}}\nabla\cdot\mathbf{u}\delta_{\nu\kappa}, \tag{11}$$

where $\mathbf{u}(\mathbf{r},\omega)=\mathbf{j}(\mathbf{r},\omega)/n_0(\mathbf{r})$ is the velocity field, and η_{xc} and ζ_{xc} are complex viscosity coefficients defined as

$$\eta_{\mathrm{xc}}(n,\omega)=-\frac{n^2}{i\omega}f_{\mathrm{xc}}^T(n,\omega), \tag{12}$$

$$\zeta_{\mathrm{xc}}(n,\omega)=-\frac{n^2}{i\omega}\left[f_{\mathrm{xc}}^L(n,\omega)-\frac{4}{3}f_{\mathrm{xc}}^T(n,\omega)-\frac{d^2e_{\mathrm{xc}}}{dn^2}\right]. \tag{13}$$

$f_{\mathrm{xc}}^L(n,\omega)$ and $f_{\mathrm{xc}}^T(n,\omega)$ are frequency-dependent xc kernels for the homogeneous electron gas, and are reasonably well known.[11,22,23] In Eq. (11), η_{xc} and ζ_{xc} are both evaluated at the local $n_0(\mathbf{r})$.

B. Excitation energies from the current–density response: Small-matrix approximation

To determine the excitation energies of the system, we search for those frequencies where there exist solutions of Eq. (1) with *finite* $\mathbf{j}(\mathbf{r},\omega)$ in the *absence* of any external perturbation.[4] These solutions can be viewed as the ''eigenmodes'' of the system. The current response equation then becomes

$$j_\mu(\mathbf{r},\omega)=\sum_\nu \int d^3r'\,\chi_{\mu\nu}(\mathbf{r},\mathbf{r}',\omega)a_\nu^{\mathrm{Hxc}}(\mathbf{r}',\omega), \tag{14}$$

where

$$a_\nu^{\mathrm{Hxc}}(\mathbf{r},\omega)=\frac{\nabla_\nu}{(i\omega)^2}\int d^3r'\nabla'\cdot\mathbf{j}(\mathbf{r}',\omega)f_{\mathrm{Hxc}}^{\mathrm{ALDA}}(\mathbf{r},\mathbf{r}') - \frac{1}{i\omega n_0(\mathbf{r})}\sum_\kappa \nabla_\kappa\sigma_{\nu\kappa}^{\mathrm{xc}}(\mathbf{r},\omega). \tag{15}$$

Equations (14) and (15) can in principle be solved numerically, for instance by generalizing Casida's technique.[3] Instead, we proceed to derive an approximation for the excitation energy involving levels p (occupied) and q (unoccupied), both of which are assumed to be nondegenerate.[24] The Kohn–Sham (KS) orbitals are taken to be real. We approximate the current–current response tensor as

$$\chi_{\mu\nu}(\mathbf{r},\mathbf{r}',\omega)\approx\frac{(i\omega)^2}{2\omega_{pq}^2}\left(\frac{1}{\omega+\omega_{pq}}-\frac{1}{\omega-\omega_{pq}}\right) \times P_\mu^{pq}(\mathbf{r})P_\nu^{pq}(\mathbf{r}'), \tag{16}$$

where $\omega_{pq}=\varepsilon_p-\varepsilon_q$, and

$$P_\mu^{pq}(\mathbf{r})=\psi_p(\mathbf{r})\nabla_\mu\psi_q(\mathbf{r})-\psi_q(\mathbf{r})\nabla_\mu\psi_p(\mathbf{r}). \tag{17}$$

We will comment later on the motivation for this approximation. Equation (15) thus becomes

$$\begin{aligned}a_\nu^{\mathrm{Hxc}}(\mathbf{r},\omega)=\frac{(i\omega)^2}{\omega_{pq}^2}\left(\frac{\omega_{pq}}{\omega_{pq}^2-\omega^2}\right)\sum_{\kappa\xi}\Bigg(&\frac{\nabla_\nu}{(i\omega)^2}\int d^3r'\,f_{\mathrm{Hxc}}^{\mathrm{ALDA}}(\mathbf{r},\mathbf{r}')\nabla'_\kappa P_\kappa^{pq}(\mathbf{r}')\int d^3r''P_\xi^{pq}(\mathbf{r}'')a_\xi^{\mathrm{Hxc}}(\mathbf{r}'',\omega)\\ &-\frac{\nabla_\kappa}{i\omega n_0(\mathbf{r})}\Bigg\{\eta_{\mathrm{xc}}(\mathbf{r},\omega)\left[\nabla_\nu\frac{P_\kappa^{pq}(\mathbf{r})}{n_0(\mathbf{r})}+\nabla_\kappa\frac{P_\nu^{pq}(\mathbf{r})}{n_0(\mathbf{r})}\right]\int d^3r'P_\xi^{pq}(\mathbf{r}')a_\xi^{\mathrm{Hxc}}(\mathbf{r}',\omega)\\ &+\left[\zeta_{\mathrm{xc}}(\mathbf{r},\omega)-\frac{2}{3}\eta_{\mathrm{xc}}(\mathbf{r},\omega)\right]\delta_{\nu\kappa}\sum_\mu\nabla_\mu\frac{P_\mu^{pq}(\mathbf{r})}{n_0(\mathbf{r})}\int d^3r'P_\xi^{pq}(\mathbf{r}')a_\xi^{\mathrm{Hxc}}(\mathbf{r}',\omega)\Bigg\}\Bigg).\end{aligned} \tag{18}$$

Operating with $\Sigma_\nu\int d^3rP_\nu^{pq}(\mathbf{r})$ on Eq. (18) allows us to cancel $H(\omega)=\Sigma_\nu\int d^3rP_\nu^{pq}(\mathbf{r})a_\nu^{\mathrm{Hxc}}(\mathbf{r},\omega)$, which leads to

$$\begin{aligned}1=\frac{(i\omega)^2}{\omega_{pq}^2}\left(\frac{\omega_{pq}}{\omega_{pq}^2-\omega^2}\right)\sum_{\kappa\nu}\int d^3rP_\nu^{pq}(\mathbf{r})&\\ \times\Bigg(\frac{\nabla_\nu}{(i\omega)^2}\int d^3r'\,f_{\mathrm{Hxc}}^{\mathrm{ALDA}}(\mathbf{r},\mathbf{r}')\nabla'_\kappa P_\kappa^{pq}(\mathbf{r}')&\\ -\frac{\nabla_\kappa}{i\omega n_0(\mathbf{r})}\Bigg\{\eta_{\mathrm{xc}}(\mathbf{r},\omega)[\nabla_\nu u_\kappa^{pq}(\mathbf{r})+\nabla_\kappa u_\nu^{pq}(\mathbf{r})]&\\ +\left[\zeta_{\mathrm{xc}}(\mathbf{r},\omega)-\frac{2}{3}\eta_{\mathrm{xc}}(\mathbf{r},\omega)\right]\delta_{\nu\kappa}\nabla\cdot\mathbf{u}_\mu^{pq}(\mathbf{r})\Bigg\}\Bigg),&\end{aligned} \tag{19}$$

where $u_\nu^{pq}=P_\nu^{pq}/n_0$ is the velocity field associated with the $p\to q$ excitation under study. We perform partial integrations, and use

$$\psi_p(\mathbf{r})\nabla^2\psi_q(\mathbf{r})-\psi_q(\mathbf{r})\nabla^2\psi_p(\mathbf{r})=2\omega_{pq}\psi_p(\mathbf{r})\psi_q(\mathbf{r}) \tag{20}$$

in the ALDA part. After some further manipulations, this leads to the following expression:

$$\begin{aligned}\omega^2=\omega_{pq}^2+2\omega_{pq}S_{pq}-\frac{i\omega}{\omega_{pq}}\int d^3r&\\ \times\Bigg\{\eta_{\mathrm{xc}}(\mathbf{r},\omega)\frac{1}{2}\sum_{\nu\kappa}[\nabla_\nu u_\kappa^{pq}(\mathbf{r})+\nabla_\kappa u_\nu^{pq}(\mathbf{r})]^2&\\ +\left[\zeta_{\mathrm{xc}}(\mathbf{r},\omega)-\frac{2}{3}\eta_{\mathrm{xc}}(\mathbf{r},\omega)\right][\nabla\cdot\mathbf{u}^{pq}(\mathbf{r})]^2\Bigg\},&\end{aligned} \tag{21}$$

where

$$S_{pq}=2\int d^3r\int d^3r'\,\psi_p(\mathbf{r})\psi_q(\mathbf{r}) \times f_{\mathrm{Hxc}}^{\mathrm{ALDA}}(\mathbf{r},\mathbf{r}')\psi_p(\mathbf{r}')\psi_q(\mathbf{r}'). \tag{22}$$

Equation (21) features a nonadiabatic correction to the well-known ALDA–SMA,

$$\omega_{\mathrm{ALDA}}^2=\omega_{pq}^2+2\omega_{pq}S_{pq}. \tag{23}$$

We can rewrite Eq. (21) as

$$\omega^2=\omega_{\mathrm{ALDA}}^2-\frac{i\omega}{\omega_{pq}}\sum_{\nu\kappa}\int d^3r\,\sigma_{\mathrm{xc},\kappa\nu}^{pq}(\mathbf{r},\omega)\nabla_\kappa u_\nu^{pq}(\mathbf{r}), \tag{24}$$

where $\sigma_{\mathrm{xc}}^{pq}$ is the xc stress tensor (11) with the exact u_ν replaced by u_ν^{pq}. For the numerical analysis later on in Sec. III B, we define the integral kernel $R^{pq}(r,\omega)$ via

TABLE I. Excitation energies (in eV) for the lowest $s \rightarrow s$ transitions in closed-shell atoms and ions.

Transition	Expt.	Bare KS	ALDA	VUC ($\mu_{xc}=0$)	VUC (finite μ_{xc})
Be $2s \rightarrow 3s$	6.779	5.564	5.622	$5.665-0.038i$	$5.669-0.037i$
B^+ $2s \rightarrow 3s$	16.812	15.166	15.490	$15.649-0.143i$	$15.664-0.127i$
B^+ $2s \rightarrow 4s$	20.821	17.760	17.826	$17.837-0.020i$	$17.840-0.017i$
Mg $3s \rightarrow 4s$	5.394	4.719	4.777	$4.823-0.047i$	$4.829-0.046i$
Al^+ $3s \rightarrow 4s$	11.822	11.182	11.409	$11.533-0.142i$	$11.558-0.127i$
Al^+ $3s \rightarrow 5s$	15.048	13.395	13.442	$13.450-0.020i$	$13.454-0.018i$
Ca $4s \rightarrow 5s$	4.131	3.765	3.814	$3.859-0.055i$	$3.865-0.055i$
Sc^+ $4s \rightarrow 5s$	8.603	8.200	8.350	$8.442-0.139i$	$8.469-0.128i$
Sc^+ $4s \rightarrow 6s$		10.065	10.095	$10.101-0.021i$	$10.106-0.019i$
Sr $5s \rightarrow 6s$	3.793	3.495	3.539	$3.582-0.058i$	$3.589-0.057i$
Y^+ $5s \rightarrow 6s$	7.609	7.313	7.436	$7.519-0.141i$	$7.545-0.131i$
Y^+ $5s \rightarrow 7s$		9.047	9.072	$9.078-0.023i$	$9.083-0.020i$

$$\int_0^\infty dr r^2 R^{pq}(r,\omega) = \frac{i\omega}{\omega_{pq}} \sum_{\nu\kappa} \int d^3r \sigma^{pq}_{\mathrm{xc},\kappa\nu}(\mathbf{r},\omega) \nabla_\kappa u^{pq}_\nu(\mathbf{r}). \tag{25}$$

The ALDA–SMA, Eq. (23), is normally derived starting from the density response equation and replacing the response function (4) by

$$\chi(\mathbf{r},\mathbf{r}',\omega) \approx 2\psi_p(\mathbf{r})\psi_q(\mathbf{r})\psi_p(\mathbf{r}')\psi_q(\mathbf{r}') \times \left(\frac{1}{\omega-\omega_{pq}} - \frac{1}{\omega+\omega_{pq}} \right), \tag{26}$$

keeping only those terms which contain that Kohn–Sham excitation ω_{pq} which we want to correct. Notice that relation (5) only holds between the *exact* density and current response functions, and should therefore not be used to derive a corresponding expression for $\chi_{\mu\nu}$ from an approximate χ, or vice versa. Instead, our approximation for $\chi_{\mu\nu}$, Eq. (16), is a direct consequence of the requirement that it reduces to the ALDA result (23) in the appropriate limit.

In classical fluid dynamics,[25] the average rate of energy dissipation per unit time in a viscous fluid is

$$\dot{E}_{\mathrm{diss}} = -\sum_{\nu\kappa} \int d^3r \sigma_{\kappa\nu} \nabla_\kappa u_\nu, \tag{27}$$

where σ is the viscoelastic stress tensor of the fluid. In deriving Eq. (27), the viscosity coefficients η and ξ are usually assumed to be real, positive constants. In our case, they are frequency dependent and complex, so the rate of energy dissipation (27) has both real and imaginary part. Assuming small nonadiabaticity, Eq. (24) becomes

$$\omega \approx \omega_{\mathrm{ALDA}} + \frac{\Im \dot{E}_{\mathrm{diss}}}{2\omega_{\mathrm{ALDA}}} - i\frac{\Re \dot{E}_{\mathrm{diss}}}{2\omega_{\mathrm{ALDA}}}, \tag{28}$$

to lowest order in $\dot{E}_{\mathrm{diss}}/\omega^2_{\mathrm{ALDA}}$. Thus, energy dissipation from xc viscoelastic stresses leads to nonadiabatic corrections to ω_{ALDA} in the form of a frequency shift and a finite linewidth.

A finite linewidth is an important physical property of collective excitations in extended systems, such as intersubband plasmons in quantum wells.[16,17] However, for bound-to-bound transitions in finite systems the linewidth should be exactly zero. This condition is difficult to satisfy for approximate xc functionals based on the electron gas, and we will see that VUC leads to atomic excitation energies with finite (but usually small) imaginary parts.

III. RESULTS AND DISCUSSION

A. Excitation energies of closed-shell atoms and ions

We now apply our formalism to calculate nonadiabatic corrections to ALDA excitation energies for closed-shell atoms and ions. To evaluate Eq. (21), one needs the viscoelastic xc stress tensor expressed in spherical polar coordinates (r,θ,ϕ). In particular, see Ref. 25 for the incompressible part of σ_{xc}. Notice further that if the excitation frequency ω acquires a finite imaginary part, analytic continuation of the xc kernels into the complex ω plane is required.[26]

In the following calculations, we have used the LDA functional of Vosko *et al.*[27] and the longitudinal and transverse xc kernels $f^L_{\mathrm{xc}}(n,\omega)$ and $f^T_{\mathrm{xc}}(n,\omega)$ in the parametrization of Qian and Vignale (QV).[23] The QV parametrization requires as input the xc energy density $e_{\mathrm{xc}}(n)$[27] and the xc shear modulus μ_{xc}[28] of a homogeneous electron gas of density n. At present, the shear modulus μ_{xc} is only approximately known for a few values in the metallic density range $1<r_s<5$ (see Table 1 in Ref. 23). We will therefore present later two different VUC results: (a) using $\mu_{\mathrm{xc}}=0$ in the QV parametrization, (b) including μ_{xc}, but only in the range $1<r_s<5$ where it is known.

We have calculated excitation energies associated with $s \rightarrow s$ and $s \rightarrow p$ singlet transitions of the closed-shell atoms Be, Mg, Ca, Sr, and the positive ions B^+, Al^+, Sc^+, Y^+. For the neutral atoms, only the lowest excitation energies were calculated. For the positive ions, LDA yields more unoccupied bound KS orbitals, which allows one to consider some additional higher excitations. The results are given in Tables I and II, showing experimental[29,30] and calculated values: ω_{pq} (bare KS), ω_{ALDA} [ALDA, Eq. (23)], and ω [VUC, Eq. (21)].

We first discuss the $s \rightarrow s$ transitions in Table I. We find in all cases that the VUC functional produces a small but noticeable improvement upon the ALDA excitation energies. The up-shift is around 1% for the lowest excitations of the neutral atoms and the ions, but less than 0.1% for the higher excitations of the ions. We also find that all excitation ener-

TABLE II. Excitation energies (in eV) for the lowest $s\rightarrow p$ transitions in closed-shell atoms and ions. The numbers in parentheses for Sr and Y^+ were calculated using Eq. (28).

Transition	Expt.	Bare KS	ALDA	VUC ($\mu_{xc}=0$)	VUC (finite μ_{xc})
Be $2s\rightarrow 2p$	5.277	3.498	5.077	$4.276-0.500i$	$6.236-0.689i$
B^+ $2s\rightarrow 2p$	9.100	5.948	8.569	$6.384-1.094i$	$11.709-1.955i$
B^+ $2s\rightarrow 3p$	17.867	16.346	16.232	$16.257-0.443i$	$16.566-0.370i$
B^+ $2s\rightarrow 4p$	21.151	18.072	18.050	$18.045-0.105i$	$18.107-0.086i$
Mg $3s\rightarrow 3p$	4.346	3.394	4.571	$4.509-0.093i$	$4.855-0.090i$
Al^+ $3s\rightarrow 3p$	7.421	5.729	7.745	$7.527-0.183i$	$8.071-0.173i$
Al^+ $3s\rightarrow 4p$	13.256	12.462	12.474	$12.648-0.128i$	$12.679-0.113i$
Al^+ $3s\rightarrow 5p$	15.606	13.744	13.748	$13.783-0.034i$	$13.790-0.030i$
Ca $4s\rightarrow 4p$	2.933	2.394	3.381	$2.962-0.063i$	$3.222-0.063i$
Sc^+ $4s\rightarrow 4p$	5.453	3.841	5.371	$4.536-0.099i$	$4.917-0.097i$
Sc^+ $4s\rightarrow 5p$		9.213	9.204	$9.334-0.121i$	$9.356-0.111i$
Sc^+ $4s\rightarrow 6p$		10.353	10.352	$10.375-0.031i$	$10.380-0.028i$
Sr $5s\rightarrow 5p$	2.690	2.215	3.105	$(-1.836-0.064i)$	$(-1.630-0.060i)$
Y^+ $5s\rightarrow 5p$	5.526	3.505	4.850	$(-3.842-0.098i)$	$(-3.522-0.088i)$
Y^+ $5s\rightarrow 6p$		8.279	8.275	$7.916-0.118i$	$7.936-0.111i$
Y^+ $5s\rightarrow 7p$		9.313	9.313	$9.211-0.035i$	$9.216-0.032i$

gies in VUC acquire an imaginary part, which is of the order of the shift of the real part. The VUC results with and without μ_{xc} are very close.

The situation is less straightforward for the $s\rightarrow p$ transitions in Table II. We observe the general trend that the VUC corrections to the ALDA excitation energies are much larger than for the $s\rightarrow s$ transitions (real as well as imaginary parts). For the positive ions, we see that the effect of the VUC functional becomes smaller for higher $s\rightarrow p$ excitations. For the lower excitations, there are pronounced differences for the case with and without μ_{xc}.

VUC often corrects the ALDA excitation energies in the right direction. Sometimes the performance is better with $\mu_{xc}=0$ (down-shift for Mg and Al^+ $3s\rightarrow 3p$), and sometimes better with finite μ_{xc} (up-shift for Be and B^+). There are cases of substantial improvement over the ALDA, in particular for Mg and Ca. On the other hand, for Be and B^+ (finite μ_{xc}) we find that VUC drastically overcorrects the ALDA. The calculation breaks down for Sr and Y^+ resulting in VUC down-shifts larger than ω_{ALDA} [the corresponding numbers in Table II were obtained from Eq. (28), since Eq. (24) would yield imaginary excitation energies in this case].

These trends are in qualitative agreement with a recent study by van Faassen and de Boeij[31] who implemented the VUC functional in benchmark studies of various molecular excitations. Their computational approach differs from ours in that they solve numerically the full current response Eqs. (14) and (15), but they ignore the imaginary part of the VUC functional. They find that VUC gives good results for $\pi^*\leftarrow\pi$ transitions, but in general fails for $\pi^*\leftarrow n$ transitions, giving strong overestimates in many cases.

B. Analysis of the VUC functional for atomic excitations

As we have seen in the previous section, going beyond the ALDA works well for some excitations, but results in overcorrections for others. In the following, we provide an analysis of the situation. There are several potential issues when applying our VUC approach to a calculation of atomic or molecular excitation energies. The first issue concerns our use of the SMA versus a full solution of the TDDFT response equation. However, this is an unlikely source for the observed VUC breakdown in some of the $s\rightarrow p$ excitations: first of all, there are no such problems in the ALDA–SMA, and second, a similar failure was observed by van Faassen and de Boeij[31] in their full calculations for molecules. Full $s\rightarrow p$ ALDA excitation energies for Be, Mg, Ca, and Sr were also calculated by Vasiliev *et al.*,[32] and all of them are lower than the ALDA–SMA by about 0.14 eV.

Next, one needs to consider the range of validity of the VUC functional itself for atomic excitations. In their original derivation based on a weakly inhomogeneous electron gas, VK[13] gave the conditions $k,q\ll k_F,\omega/v_F$, where k_F and v_F are the local Fermi wave vector and velocity, respectively. k is a measure for the degree of nonuniformity of the ground-state density, and we can rewrite the associated condition as

$$\frac{|\nabla n_0|}{n_0}\ll k_F,\omega/v_F. \tag{29}$$

On the other hand, q measures the degree of spatial variation of the external perturbation. For finite systems like atoms and molecules, one needs to consider instead the spatial variation of the current response, so that

$$\left|\frac{\nabla j_\nu}{j_\nu}\right|\ll k_F,\omega/v_F. \tag{30}$$

With the velocity profile defined as $\mathbf{u}=\mathbf{j}/n_0$, conditions (29) and (30) also imply

$$\left|\frac{\nabla u_\nu}{u_\nu}\right|\ll k_F,\omega/v_F. \tag{31}$$

Conditions (30) and (31) require that the gradients of the current and velocity fields are small, in order for the hydrodynamic VUC approach to be applicable. This indicates a largely collective motion of the electron liquid, with only little internal compression.

It turns out that none of the conditions (29)–(31) is particularly well satisfied for atoms. Close to the nucleus, the

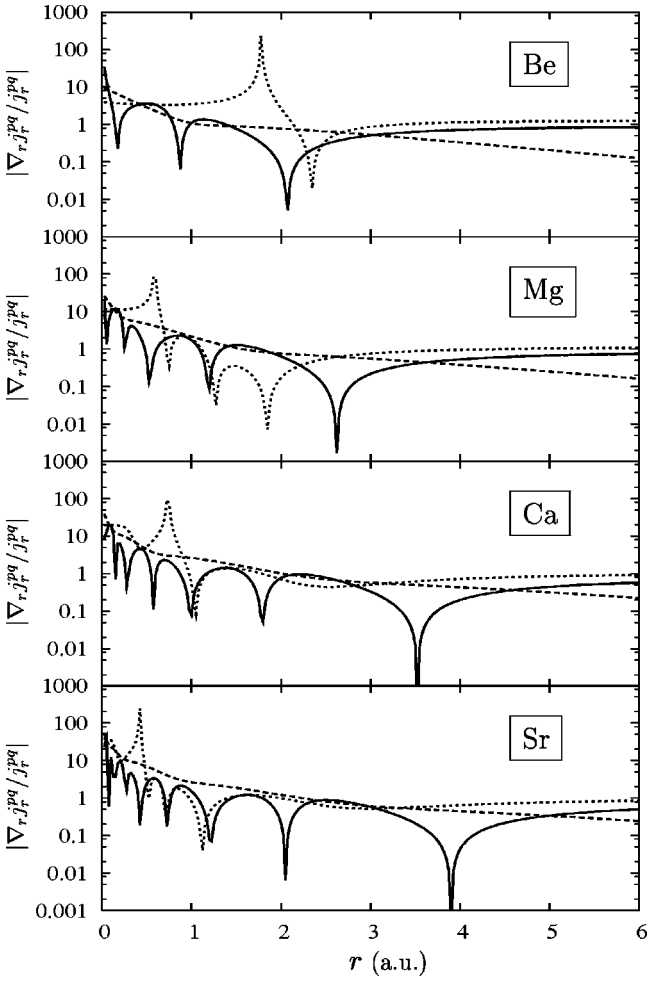

FIG. 1. Test of criterion (30) for Be, Mg, Ca, and Sr. Dashed lines: local k_F. Full and dotted lines: $|\nabla_r j_r^{pq}/j_r^{pq}|$ for $s\rightarrow s$ and $s\rightarrow p$ excitations.

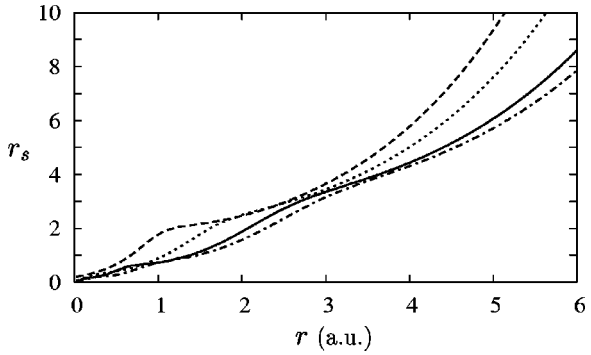

FIG. 2. LDA Wigner–Seitz radius r_s for Be (long-dashed line), Mg (dotted line), Ca (full line), and Sr (dash-dotted line).

ground-state densities change quite rapidly, so that $|\nabla n_0|/n_0$ is typically of the same order or larger than the local k_F (the condition involving ω/v_F is easily satisfied in the inner atomic region).

The conditions involving j_ν and u_ν depend on the particular kind of excitation under consideration. In general, condition (30) is better satisfied for the $s\rightarrow s$ than for the $s\rightarrow p$ transitions. This is illustrated in Fig. 1, where we plot $|\nabla_r j_r^{pq}/j_r^{pq}|$ and k_F for the $s\rightarrow s$ and $s\rightarrow p$ excitations. In the former case, the criterion (30) is quite well satisfied. However, for $s\rightarrow p$ excitations we find a sharp peak around $r=1.8$ a.u. (Be) and $r=0.4$–0.6 a.u. (Mg, Ca, Sr), which means that Eq. (30) is strongly violated. The reason for this sharp peak is that the radial current associated with $s\rightarrow p$ excitations reverses direction between atomic shells and in doing so passes through zero, so that $|\nabla_r j_r^{pq}/j_r^{pq}|$ becomes infinite. A similar behavior occurs for the polar currents j_θ^{pq} (which are absent for the strictly radial $s\rightarrow s$ excitations).

We now direct our attention to the fact that the VUC functional requires the longitudinal and transverse xc kernels $f_{\rm xc}^L(n,\omega)$ and $f_{\rm xc}^T(n,\omega)$ of the homogeneous electron gas as input, which are only approximately known. We have recalculated the excitation energies in Tables I and II using the parametrization of Nifosi *et al.*,[22] and we find that for the $s\rightarrow p$ excitations the results get slightly worse in the sense that we obtain even stronger overestimates. The QV parametrization,[23] which satisfies exact constraints for $f_{\rm xc}^L(n,\omega)$ and $f_{\rm xc}^T(n,\omega)$ in the low-frequency limits, seems to give overall better results.

As discussed earlier, the QV parametrization relies in part on the xc shear modulus $\mu_{\rm xc}$, which is available only for few values of the Wigner–Seitz radius r_s between 1 and 5. While this is normally sufficient to describe systems in the metallic density range, atomic densities are much higher near the nucleus, which means that the region of $r_s\sim 0.1$ becomes important. This is illustrated Fig. 2, which shows r_s for Be, Mg, Ca, and Sr. Our results in Tables I and II were calculated setting $\mu_{\rm xc}=0$ in those regions with $r_s<1$, which is of course a potential source for errors. It therefore remains a very important task to develop parametrizations for $f_{\rm xc}^L(n,\omega)$ and $f_{\rm xc}^T(n,\omega)$ that are accurate over the wide density range occurring in atoms and molecules.

Indeed, our insufficient knowledge of the xc kernels is another likely reason why the VUC functional performs progressively worse for heavier atoms and ions, for the case of $s\rightarrow p$ excitations. To confirm this diagnosis, and to illustrate the importance of a more accurate treatment of the high-density regions, we plot in Figs. 3 and 4 the essential ingredients of the nonadiabatic VUC correction formula for the excitation energies, Eq. (24).

Figure 3 shows the radial derivatives of the radial component of the velocity field, $|\nabla_r u_r^{pq}|$, associated with the lowest $s\rightarrow s$ and $s\rightarrow p$ excitations. Derivatives of the velocity field enter quadratically in Eq. (24), weighted with the viscosity coefficients $\eta_{\rm xc}$ and $\zeta_{\rm xc}$. One clearly sees that the $s\rightarrow p$ transitions have much larger values of $|\nabla_r u_r^{pq}|$ (and in addition, there are also components and derivatives along θ, which are absent for the $s\rightarrow s$ transitions). This suggests that the large VUC frequency shifts for the $s\rightarrow p$ excitations arise predominantly from contributions in the high-density region close to the nucleus. This region has a much smaller weight for the $s\rightarrow s$ excitations, because the velocity gradients are much smaller.

Figure 4 shows the real part of the radial integrand of the VUC correction, $r^2R^{pq}(r,\omega)$ [Eq. (25)], evaluated with finite $\mu_{\rm xc}$ and at $\omega_{\rm ALDA}$. For the two types of excitation, very different spatial regions contribute to the VUC correction: the outer region ($r>5$ a.u.) for $s\rightarrow s$, and the region close to

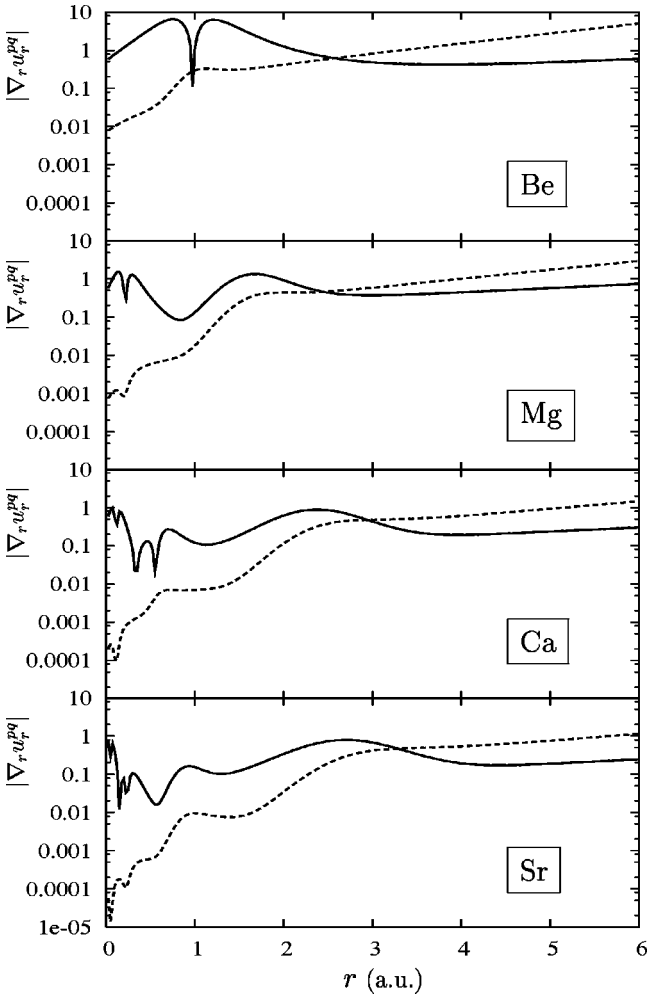

FIG. 3. Radial derivative of the radial component of the velocity field, $|\nabla_r u_r^{pq}|$, for the lowest $s\rightarrow s$ (dashed lines) and $s\rightarrow p$ (full lines) excitations of Be, Mg, Ca, and Sr.

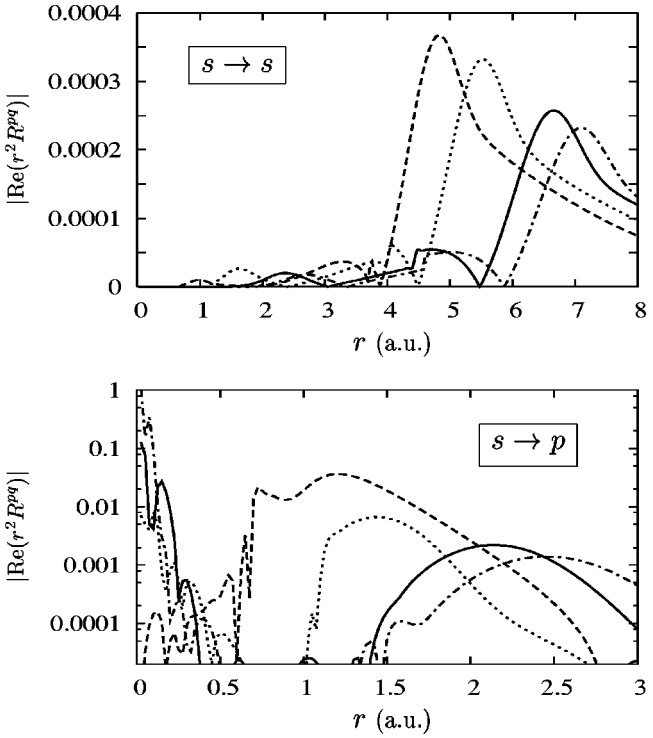

FIG. 4. $|\mathrm{Re}(r^2R^{pq})|$ [Eq. (25)] for the $s\rightarrow s$ and $s\rightarrow p$ transitions of Be (long-dashed line), Mg (dotted line), Ca (full line), and Sr (dash-dotted line).

the nucleus for $s\rightarrow p$ (notice the logarithmic scale). The broad hump for Be around $r_s=1$, which produces a positive frequency shift, rapidly decreases and moves to the right for the heavier atoms. The dominant contributions for the $s\rightarrow p$ excitations in Ca and Sr, associated with frequency downshifts, take place for $r_s<1$ (see Fig. 2). This again points out the need for a more accurate parametrization of $f_{\mathrm{xc}}^L(n,\omega)$ and $f_{\mathrm{xc}}^T(n,\omega)$ in that region.

IV. CONCLUSION

The goal of this work was to gain deeper insight into the nature of nonadiabatic effects beyond the ALDA in the calculation of excitation energies with TDDFT. Such effects are best described in the framework of linear current–density response, using the linearized xc vector potential first derived by VK[13] and later recast in the language of hydrodynamics by VUC.[14] This approach has met with recent success in calculating axial polarizabilities of molecular chains,[19,20] but appears to perform inconsistently for molecular excitations.[31]

Starting from the full current–density response equation, we have derived a simplified approach for calculating VUC excitation energies, which can be viewed as a generalization of the so-called small-matrix approximation.[5] This formalism is appealing because if features an explicit and relatively simple expression for the nonadiabatic VUC corrections on top of the ALDA excitation energies. Furthermore, our approach allows for an intuitive physical interpretation for nonadiabatic frequency shifts in terms of the average rate of energy dissipation induced by the xc viscosity of the electron liquid.

Our calculations of excitation energies for various closed-shell atoms and ions show that the VUC approach works for some excitations (namely, $s\rightarrow s$), but has problems for others ($s\rightarrow p$). A detailed analysis identifies two likely causes for the observed difficulties.

(1) The VUC functional is formally justified only if the system under consideration has a slowly varying ground-state density, and if the currents associated with a particular excitation are also slowly varying on the scale of the local k_F. These conditions are often not too well satisfied in practice, and sometimes even severely violated. Of course, our experience with the LDA in ground-state DFT shows that a method may be very successful in practice even though it is not very well formally justified. Thus, one cannot say with certainty that VUC always breaks down if conditions (29)–(31) are violated. However, our comparison of $s\rightarrow s$ and $s\rightarrow p$ excitations suggests that these criteria nevertheless provide some useful guidance, in particularly if the violation is very strong (i.e., involving a singularity).

(2) The VUC functional requires the complex, frequency-dependent xc kernels f_{xc}^L and f_{xc}^T of the homogeneous electron gas as input, which are only approximately known. The last few years have witnessed steady progress in constructing better parametrizations for the xc kernels, but

clearly more work is required. This is especially important in the high-density region ($r_s<1$), which often makes the largest contribution to the nonadiabatic corrections.

Since the VUC functional is based on the frequency-dependent xc kernel of the homogeneous electron gas, it produces excitation energies with small but finite imaginary parts. The requirement that excitation energies of bound-to-bound transitions in finite systems be real imposes an additional constraint on any approximate, frequency-dependent xc vector potential, which will be the subject of future study. We also mention that the VUC formalism in its full implementation[3,31] may produce oscillator strengths with small imaginary parts (which should, however, satisfy the f-sum rule since particle conservation is guaranteed). One can show that within the VUC–SMA of the present paper one obtains the (real) Kohn–Sham oscillator strengths.

In summary, the VUC approach shows much promise for the calculation of excitation energies for atomic and molecular systems, as well as for plasmon-like excitations in solids and nanostructures. The specific question of the applicability and of possible improvements of the VUC functional, and the more general question of the importance and significance of nonadiabatic effects in electron dynamics, merit further study.

ACKNOWLEDGMENTS

C.A.U. acknowledges support by the donors of the Petroleum Research Fund, administered by the ACS, and by the University of Missouri Research Board. K.B. was supported by DOE under Grant No. DE-FG02-01ER45928. The authors thank M. van Faassen, P. L. de Boeij, and G. Vignale for discussions.

[1] E. Runge and E. K. U. Gross, Phys. Rev. Lett. **52**, 997 (1984).
[2] E. K. U. Gross, J. F. Dobson, and M. Petersilka, in *Density Functional Theory II*, *Topics in Current Chemistry*, Vol. 181 (Springer, Berlin, 1996), p. 81.
[3] M. E. Casida, in *Recent Advances in Density Functional Methods*, edited by D. P. Chong (World Scientific, Singapore, 1995), p. 155.
[4] M. Petersilka, U. J. Gossmann, and E. K. U. Gross, Phys. Rev. Lett. **76**, 1212 (1996).
[5] H. Appel, E. K. U. Gross, and K. Burke, Phys. Rev. Lett. **90**, 043005 (2003).
[6] F. Furche and R. Ahlrichs, J. Chem. Phys. **117**, 7433 (2002).
[7] H. M. Vaswani, C. P. Hsu, M. Head-Gordon, and G. R. Fleming, J. Phys. Chem. B **107**, 7940 (2003).
[8] M. A. L. Marques, X. Lopez, D. Varsano, A. Castro, and A. Rubio, Phys. Rev. Lett. **90**, 258101 (2003).
[9] N. T. Maitra, K. Burke, H. Appel, E. K. U. Gross, and R. van Leeuwen, in *Reviews in Modern Quantum Chemistry: A Celebration of the Contributions of R. G. Parr*, edited by K. D. Sen, (World Scientific, Singapore, 2001).
[10] A. Zangwill and P. Soven, Phys. Rev. A **21**, 1561 (1980).
[11] E. K. U. Gross and W. Kohn, Phys. Rev. Lett. **55**, 2850 (1985).
[12] J. F. Dobson, Phys. Rev. Lett. **73**, 2244 (1994).
[13] G. Vignale and W. Kohn, Phys. Rev. Lett. **77**, 2037 (1996).
[14] G. Vignale, C. A. Ullrich, and S. Conti, Phys. Rev. Lett. **79**, 4878 (1997).
[15] C. A. Ullrich and G. Vignale, Phys. Rev. B **65**, 245102 (2002).
[16] C. A. Ullrich and G. Vignale, Phys. Rev. B **58**, 15756 (1998).
[17] C. A. Ullrich and G. Vignale, Phys. Rev. Lett. **87**, 037402 (2001).
[18] I. D'Amico and G. Vignale, Phys. Rev. B **59**, 7876 (1999).
[19] M. van Faassen, P. L. de Boeij, R. van Leeuwen, J. A. Berger, and J. G. Snijders, Phys. Rev. Lett. **88**, 186401 (2002).
[20] M. van Faassen, P. L. de Boeij, R. van Leeuwen, J. A. Berger, and J. G. Snijders, J. Chem. Phys. **118**, 1044 (2003).
[21] O. V. Gritsenko, S. J. A. van Gisbergen, A. Görling, and E. J. Baerends, J. Chem. Phys. **113**, 8478 (2000).
[22] R. Nifosi, S. Conti, and M. P. Tosi, Phys. Rev. B **58**, 12758 (1998).
[23] Z. Qian and G. Vignale, Phys. Rev. B **65**, 235121 (2002).
[24] A generalization to degenerate KS orbitals is formally straightforward but unnecessary for $s\rightarrow p$ excitations in closed-shell atoms: due to symmetry, one obtains the same results from the nondegenerate formalism with any one of the p orbitals.
[25] L. D. Landau and E. Lifshitz, *Mechanics of Fluids*, Course of Theoretical Physics, Vol. 6 (Pergamon, Oxford, 1987).
[26] J. F. Dobson, G. H. Harris, and A. J. O'Connor, J. Phys.: Condens. Matter **2**, 6461 (1990).
[27] S. H. Vosko, L. Wilk, and M. Nusair, Can. J. Phys. **58**, 1200 (1980).
[28] S. Conti and G. Vignale, Phys. Rev. B **60**, 7966 (1999).
[29] C. E. Moore, Natl. Stand. Ref. Data Ser. (U.S., Natl. Bur. Stand.) **35**, Vol. I–III (1971).
[30] S. Bashkin and J. D. Stoner, *Atomic Energy Levels and Grotrian Diagrams* (North-Holland, Amsterdam, 1975).
[31] M. van Faassen and P. L. de Boeij, J. Chem. Phys. **120**, 8353 (2004).
[32] I. Vasiliev, S. Öğüt, and J. R. Chelikowsly, Phys. Rev. Lett. **82**, 1919 (1999).